

The role of hematite–ilmenite solid solution in the production of magnetic anomalies in ground- and satellite-based data

Gunther Kletetschka^{a,b,*}, Peter J. Wasilewski^b, Patrick T. Taylor^c

^a*Catholic University of America, Washington, DC, USA*

^b*Code 691, NASA/Goddard Space Flight Center, Greenbelt, MD, 20771, USA*

^c*Code 921, NASA/Goddard Space Flight Center, Greenbelt, MD, 20771, USA*

Received 5 July 2000; accepted 24 August 2001

Abstract

Remanent magnetization (RM) of rocks with hematite–ilmenite solid solution (HISS) minerals, at all crustal levels, may be an important contribution to magnetic anomalies measured by ground and satellite altitude surveys. The possibility that lower thermal gradient relatively deep in the crust can result in exsolution of HISS compositions with strong remanent magnetizations (RM) was studied for two bulk compositions within the HISS system. Samples from granulite-terranes around Wilson Lake, Labrador, Canada contain titanohematite with exsolved ferrian ilmenite lamellae. Other samples from the anorthosite-terranes of Allard Lake, Quebec, Canada contain ferrian ilmenite with exsolved titanohematite lamellae. In both cases, the final exsolved titanohematite has similar Ti content and carries dominant magnetic remanence with REM (=NRM/SIRM, where NRM is the natural remanent magnetization and SIRM is the saturation isothermal remanent magnetization) that is comparable to the Ti-free end member. The RM was acquired prior to exsolution and the ilmeno-hematite-rich rock possesses thermal remanent magnetization (TRM), whereas rocks with hemo-ilmenite possess chemical remanent magnetization (CRM). In both cases, we found fairly large homogeneous grains with low demagnetizing energy that acquired intense RM. The magnetism of the ilmeno-hematite solid solution phases is not significantly perturbed by the continuous reaction: ilmeno-hematite \rightleftharpoons titanohematite solid solution. Hence, the occurrence of HISS in rocks that cooled slowly in a low intensity magnetic field will have an intense magnetic signature characterized by a large REM. © 2002 Elsevier Science B.V. All rights reserved.

Keywords: Magnetic petrology; Hematite; Ilmenite; REM; TRM; CRM; Magnetic anomalies

1. Introduction

Large volumes of the terrestrial crust must have a significant contrast in magnetization in order to be detected at satellite altitude (i.e. 400 km). Modelling MAGSAT data has revealed that a significant magnet-

ization of the lower crust is required (Mayhew and Johnson, 1987; Schlinger, 1985; Toft and Haggerty, 1986; Wasilewski and Mayhew, 1992; Wasilewski et al., 1979). In regions with significant magnetization, the oxide mineral concentration must be enhanced and/or the remanence must contribute substantially to the anomaly signature.

Total magnetization contrasts inferred from modelling satellite altitude crustal anomalies (4–6 A/m) are larger than the induced value (0–1 A/m), which may be attributed to exposed upper crustal rocks (Mayhew

* Corresponding author. Code 691, NASA/Goddard Space Flight Center, Greenbelt, MD, 20771, USA. Tel.: +1-301-286-3804; fax: +1-301-286-0212.

E-mail address: gunther.kletetschka@gsfc.nasa.gov (G. Kletetschka).

et al., 1985; Langel, 1985). In the lower crust, either the remanent magnetization (RM) is significant or the concentration of inducing magnetic mineralogy is considerably larger than that observed at the surface. Previously, the most common carrier of the total magnetization in the mid to lower crust has been assumed to be the induced magnetization associated with multi-domain (MD), relatively pure magnetite (Schlinger, 1985; Williams et al., 1985; Shive and Fountain, 1988; Wasilewski and Warner, 1988; Reeves, 1989; Kelso et al., 1993). In this report, we consider the possibility that RM from hematite–ilmenite solid solution (HISS) mineralogy may be an important component of the total magnetization of the crust.

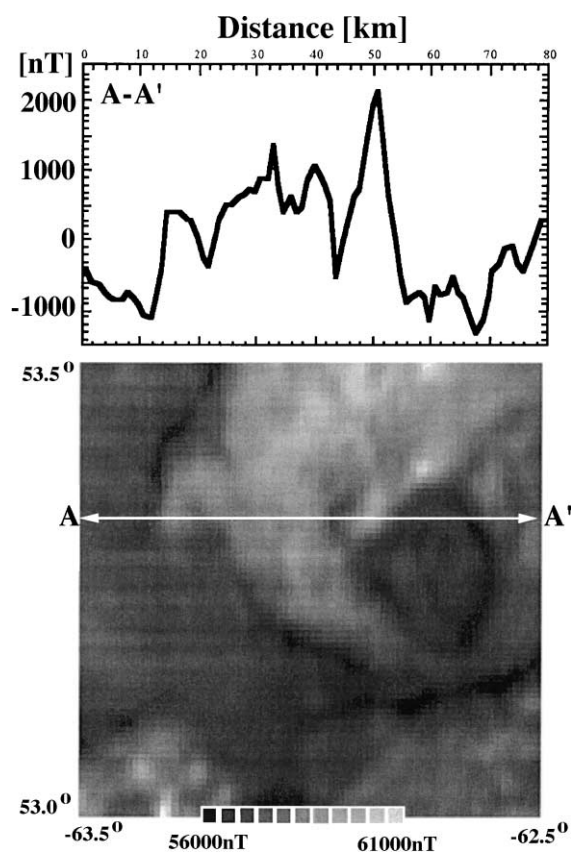


Fig. 1. Example of magnetic anomaly generated entirely by the remanent magnetism of titanohematite. The area shown is from Wilson Lake region, Labrador, Canada, which was flown at 1000-m altitude (Geological Survey of Canada, Aeromagnetic Database). Latitude is north and longitude is west of Greenwich.

For example, Kletetschka and Stout (1998) found a region (Fig. 1) where the magnetization contrast was mainly due to RM carried by HISS mineralogy. In most cases, induced magnetization contrasts reflect the relative proportions of magnetite, which has a mass susceptibility three to four orders of magnitude larger than hematite and most of the other oxides in the rocks, with the exception of maghemite. If RM is important in the mid to lower crust, then conditions must be such that minerals are produced with compositions and/or grain sizes that permit significant RM.

Mid to deep crustal rocks have been found to contain HISS (e.g. Frost and Lindsley, 1991; Frost et al., 1991; Kletetschka and Stout, 1998; Kletetschka, 1998; McEnroe and Brown, 2000; McEnroe, 1997). These samples probably involve highly oxidized sedimentary protolith. It would appear that continuous reactions, due to slow cooling, follow the miscibility gap and are responsible for the similar composition of final exsolved phases, titanohematite and ferrian ilmenite. Recently, Kletetschka et al. (2000a,b) noted that the coarse-grained (>0.1 mm) Ti-free end member of HISS could acquire intense magnetization (500–1000 A/m) when cooled in the Earth's field (~ 0.05 mT). The purpose of this work is to see if intense magnetization prevails in titanohematites and if the exsolution process interferes with the acquisition and maintenance of the intense remanence.

Titanohematite can occur in rock types that have been slowly cooled or subjected to retrograde metamorphism in relatively oxidizing conditions. Some mafic rocks in granulite and amphibolite-facies terranes have been shown to have somewhat oxidized HISS series minerals (McEnroe and Brown, 2000; McEnroe, 1997; Kletetschka, 1998; Kletetschka and Stout, 1998; Arima et al., 1986; Thomas, 1993; Schlinger and Veblen, 1989; Brown and Raith, 1985; Peretti and Köpel, 1986; Banno and Kanehira, 1961; Kanehira et al., 1964) and they contribute significantly to the remanence intensity.

Throughout this report, the terms hemo-ilmenite and ilmeno-hematite are adopted for unmixed grains that are rich in ilmenite and hematite content, respectively. In addition, titanohematite and ferrian ilmenite are used for the individual exsolved phases.

2. Materials and methods

We used a set of ilmenite samples (see Table 1) from the Allard Lake anorthosite suite, located in a region known to contain numerous outcrops of massive ilmenite enclosed in Grenville-type anorthosite of pre-Cambrian age (Hargraves and Burt, 1967; Carmichael, 1959, 1961, 1964; Hargraves, 1959). Compositional variations within the region were found in samples taken from three cores (5 cm long and 2.5 cm in diameter). Fragments from these cores are labeled a, b and c (e.g. 71a-a, 71a-b, 71a-c). Ferrian ilmenites with titanohematite exsolution lamellae were the main magnetic minerals.

The ilmenite deposits are located in an irregular sheet-like body of essentially massive hemo-ilmenite. Ore occurs in pure anorthosite with local hypersthene-rich zones overlain by coarsely banded hemo-ilmenite and anorthosite (Hammond, 1952). The hemo-ilmenite ore contains 2–3% MgO and about 1% MnO, with

a bulk composition close to 71% ilmenite (Hargraves, 1959). Magnetite is rare in these deposits.

Other samples (Table 1) from the granulite terrane at Wilson Lake, Labrador, contain titanohematite (~1% MgO) with ferrian ilmenite exsolution lamellae. The granulite terrane consists mainly of quartz-feldspathic gneisses. The thickness of the individual bands in the gneisses is quite variable (usually 0.2–2.0 cm), and the average grain size is generally 1–5 mm. Well-developed platy minerals are usually not present. Compositional banding results from the segregation of layers of dark and light minerals. Many specimens show evidence of cataclastic deformation indicated by strained quartz and feldspar grains, granulation of grain margins, and granulation zones that are generally parallel to the compositional banding (cataclastic textures). True mylonitic bands have been produced locally. The mineralogy of these granulites is relatively simple. Assemblages are combinations of quartz, plagioclase, cordierite, microcline, hypersthene, sillimanite, iron oxides (hemo-ilmenite, magnetite), biotite, sapphirine, spinel, and garnet. Layers of light materials are composed of quartz, plagioclase and microcline, quartz and plagioclase, or quartz and microcline. Quartz commonly occurs as lenticular segregations within these layers. Dark minerals are composed of combinations of hypersthene, sillimanite, iron oxides, and less commonly, sapphirine.

These granulite samples were used to show the relationship between high remanence and aeromagnetic anomalies in the Wilson Lake area (Kletetschka, 1998; Kletetschka and Stout, 1998). Microprobe compositions of pure titanohematite were difficult to establish due to the high density of exsolved ilmenite lamellae. Thus, the amount of Ti residing in the remanence carrying titanohematites (Table 1) was estimated from thermal demagnetization curves. These estimates are possible because the blocking temperatures of the minerals coincide with compositionally dependent Curie temperatures (Kletetschka et al., 2000b).

Recent studies on hematite (Kletetschka et al., 2000a,b) show that coarse-grained samples can acquire intense thermoremanent magnetization. Indeed, the grains may acquire remanence levels that are more than 50% of their saturation isothermal remanent magnetization (SIRM). This could be due to the weaker influence of demagnetizing energy relative to the wall pinning energy at temperatures approaching the Curie

Table 1
Localities and Ti content (expressed in % ilmenite) in titanohematite found in the samples used for this study

Name	Locality	% Ilmenite
71a-a	Allard Lake	11
71a-b	Allard Lake	10
71a-c	Allard Lake	11
86a-a	Allard Lake	13
86a-b	Allard Lake	13
86a-c	Allard Lake	12
112b-a	Allard Lake	10
112b-b	Allard Lake	10
112b-c	Allard Lake	11
S1a	Wilson Lake	10
S3a	Wilson Lake	9
S4b	Wilson Lake	8
S5a	Wilson Lake	12
S8a	Wilson Lake	8
S11b	Wilson Lake	11
w6b	Wilson Lake	9
1 mm	Wilson Lake	9
0.5 mm	Wilson Lake	9
0.2 mm	Wilson Lake	9
0.1 mm	Wilson Lake	9
0.05 mm	Wilson Lake	9
0.001 mm	Wilson Lake	9
w6b-1	Wilson Lake	14
w6b-2	Wilson Lake	12
w6b-3	Wilson Lake	7.5
w6b-4	Wilson Lake	6.5
w6b-5	Wilson Lake	6

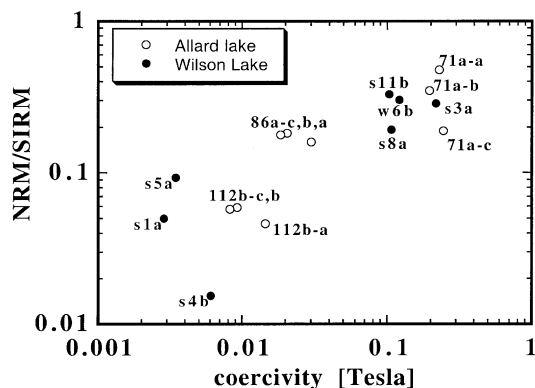


Fig. 2. REM (NRM/SIRM) for samples from the Allard Lake ilmenite deposit and the Wilson Lake hemo-ilmenite bearing granulite terrane, Labrador, Canada.

point (Kletetschka et al., 2000b). The enhanced remanence of coarse-grained samples is expressed through a large (>0.1) REM ratio. The REM value is much lower for magnetite-bearing rocks (Wasilewski and Dickinson, 2000; Wasilewski and Kletetschka, 1999), and thus, we used the REM ratio as an indicator of the presence of coarse-grained hematite.

To further characterize the grain size dependence of thermal remanent magnetization (TRM), sample w6b (massive titanohematite ore) from Central Labrador (Kletetschka, 1998) was studied. This sample

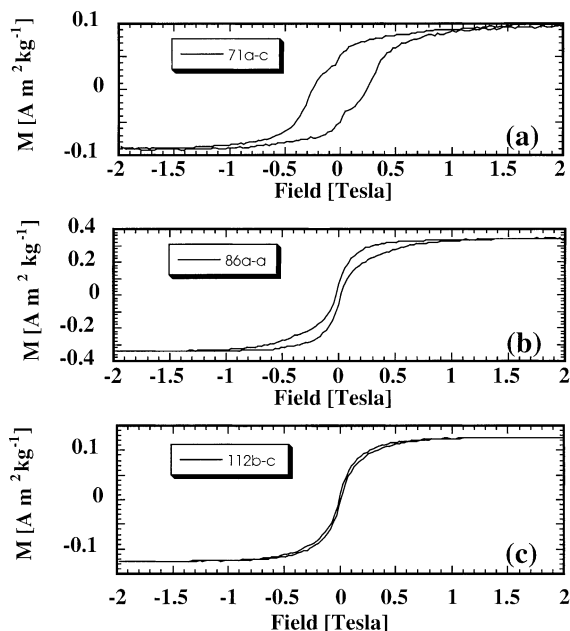


Fig. 4. Hysteresis loops of three ilmenohematite-bearing samples: (a) sample with no observable magnetite; (b) sample with a small amount (1–2%) of magnetite present; and (c) sample with significant amount of magnetite present (40–60%) (see Fig. 7B). Analyses of samples with higher magnetite content (e.g. S5a, S1a, and S4b) indicated negligible variations in their hysteresis parameters.

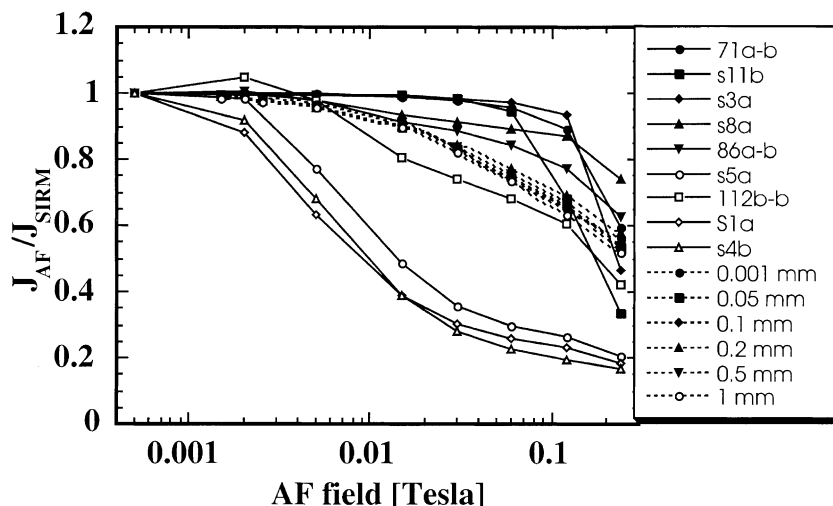


Fig. 3. Alternating field (AF) demagnetization of SIRM applied to selected titanohematite-bearing samples. Dashed curves give the effects for the w6b sample of titanohematite that was artificially crushed to various grain sizes.

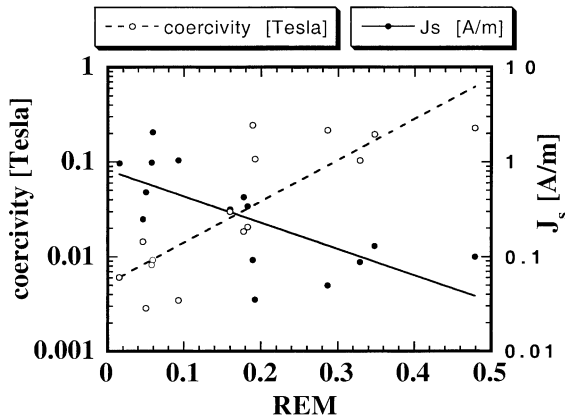


Fig. 5. General trends in coercivity and saturation magnetization (J_s) with REM for titanohematite-bearing rocks.

was crushed and sifted to obtain average grain size fractions of 1, 0.5, 0.2, 0.1 and 0.05 mm, using USA standard testing sieves with openings of 850, 250, 150, 75 and 38 μm , respectively. In addition to establishing the REM ratio for these samples, alternating field (AF) demagnetization and hysteresis properties were obtained in order to establish the relationships between the large REM values and the hysteresis parameters. Techniques used to measure the

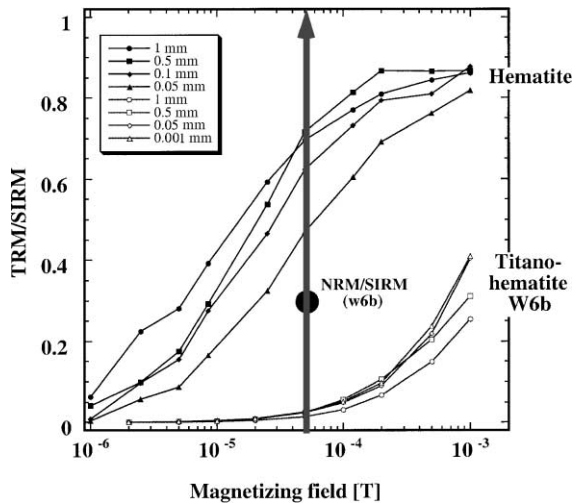


Fig. 6. TRM acquisition of pure hematite (after Kletetschka et al., 2000b) and exsolved titanohematite w6b (Fig. 7) for different grain sizes. The thick arrow indicates the Earth's magnetic field. Large solid circle on the arrow indicates the REM value for the original uncrushed w6b sample.

natural remanent magnetization (NRM) of these samples are presented in Appendix A.

3. Results

Titanohematite REM values are shown in Fig. 2. They vary between 0.50 and 0.01 and increase with coercivity for both Allard Lake anorthosite and Wilson Lake granulite. Consequently, samples were selected for AF demagnetization (Fig. 3) and magnetic hysteresis in order to establish the characteristics of the high REM samples.

The samples with high REM values were most resistant to demagnetization and held most of their remanence even when a 0.1 T AF was applied, while

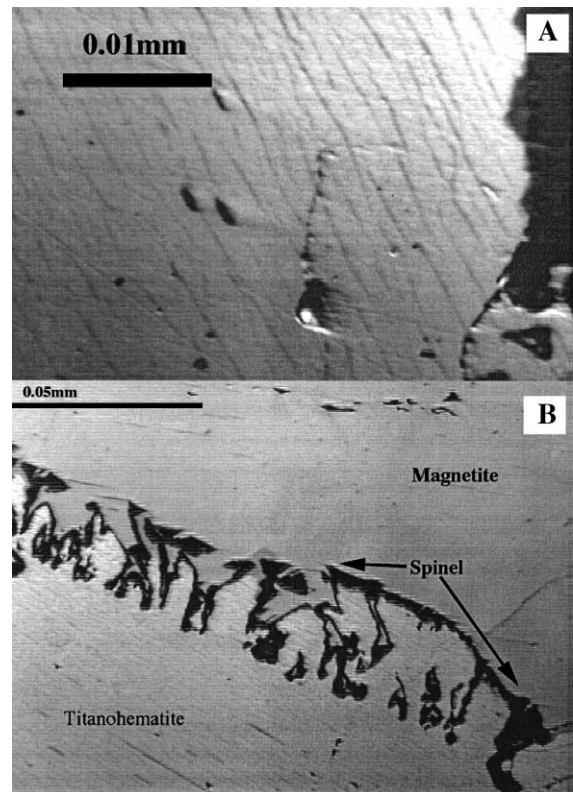


Fig. 7. Photomicrographs of w6b showing exsolution of titanohematite: (A) exsolved ilmenite lamellae within the titanohematite host, (B) symplectic intergrowth between grain exsolved titanohematite (lower left corner) and magnetite (upper right corner). The dark phase is a spinel.

low REM samples started to lose their remanence in fields above 0.002 T. Sample w6b (Wilson Lake) displayed no grain size variation during demagnetization, establishing the microstructural origin of the stability of the remanence.

Fig. 4 shows our results for three of the samples with contrasting REM properties. Clearly, samples with large REM are basically AF-resistant and have high coercivity (sample 71a-c, Allard Lake). Samples with identical REM, but containing magnetite, show constricted loops (sample 86a-a, Allard Lake) that suggest the presence of at least two phases with contrasting coercivity behavior (Wasilewski, 1973). Samples with REM values near 0.05 (e. g. 112b-c, Allard Lake) have low coercivity, while those with low coercivity values (e.g., S1a, S4b, S5a) have hysteresis properties that are almost identical with 112b-c in Fig. 4. All samples with magnetite have REM of <0.1.

These large REM values seem to be unique (Kletetschka et al., 2000a,b), and can be interpreted only by assuming the presence of coarse-grained hematite and/or by a contamination due to an intense magnetic field (Wasilewski and Kletetschka, 1999). Variation of REM with coercivity and saturation magnetization (Fig. 5) indicates that low REM samples contain significant magnetite components, and thus, low coercivities and high saturation magnetizations (J_s). Samples containing significant titanohematite have large REMs, high coercivities, and low J_s (for pure magnet-

ite, $J_s=95 \text{ A m}^2 \text{ kg}^{-1}$, while for pure hematite, $J_s=0.4 \text{ A m}^2 \text{ kg}^{-1}$).

Various grain size fractions of sample w6b, which possesses a large REM (0.3), were thermally demagnetized from above 700 °C by cooling in a shielded oven in an approximately 500 nT residual axial magnetic field. Fractions were reheated and cooled in various fields to determine the field dependence of acquisition relative to the SIRM (Fig. 6). TRM acquisition curves for all of the sized fractions of w6b follow a narrow distribution trend with negligible grain size dependence. Values of TRM, acquired at an Earth-like field ($5 \times 10^{-5} \text{ T}$ and REM=0.02–0.06), are much lower than the original NRM (REM=0.3) of the bulk sample, and this is also indicated in Fig. 6.

The contrast between the REM (0.02–0.06) produced by this reacquisition experiment and the original REM (0.3) prompted us to initiate detailed electron and optical microscopy investigations to further characterize the magnetic mineralogies of these samples. Titanohematite-rich samples were observed to contain exsolution of ferrian ilmenite lamellae, effectively dividing the titanohematite-rich grain (Fig. 7A). Titanohematite-rich grains were also commonly associated with magnetite (Fig. 7B). Hence, the magnetic character of these rocks is likely to be quite heterogeneous on a small scale, such as those that were observed by thermally demagnetizing the NRM of subsamples of sample w6b. This sample was fragmented into five

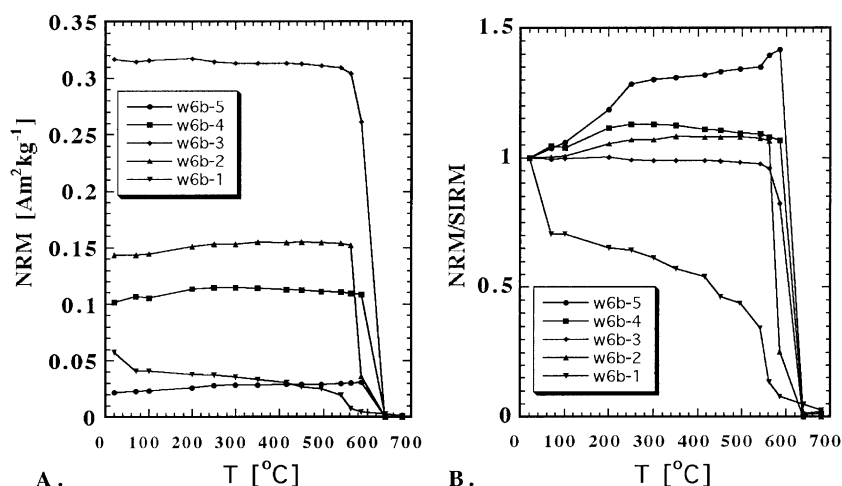


Fig. 8. (A) Thermal demagnetization of five chips of sample w6b. (B) Same data as in (A), but normalized by SIRM.

pieces (w6b-1, w6b-2, w6b-3, w6b-4 and w6b-5) of about 2–5 mm in diameter. The thermal demagnetization curves of these chips (Fig. 8A) indicated large variations in NRM ($0.02\text{--}0.31\text{ A m}^2\text{ kg}^{-1}$), as well as variation in the nature of the demagnetization (Fig. 8B).

4. Discussion

4.1. Localization of the remanence

In samples of hemo-ilmenite ore from Allard Lake (Carmichael, 1961, 1959), the RM was carried by very fine lamellae of titanohematite ($<5\text{ }\mu\text{m}$) within the ferrian ilmenite host. In these earlier studies with the ferrian ilmenite-rich ore 12N, HCl was used to perform a series of dissolution experiments on slabs of variable thickness. Etching slabs with thickness of 0.4 mm produced an 88% loss of initial magnetization, whereas for 0.2-mm thick slabs, 99.6% of the initial magnetization was lost after etching (see Table 3 in Carmichael, 1961).

The size of the titanohematite lamellae dissolved in the slab of particular thickness must be comparable with the thickness of that slab to have the entire volume of the titanohematite lamellae dissolved. Most of the very fine lamellae of titanohematite were completely enclosed within the ferrian ilmenite matrix. The fine lamellae could not hold significant RM because they were still present in the rock and separated from the acid by an ilmenite matrix after most of the original RM was lost due to dissolution of the large lamellae. Thus, most of the magnetic remanence of the Allard Lake ferrian ilmenite in Carmichael's work, and by analogy, also in our samples, must be due to large titanohematite lamellae hosting the smaller ilmenite lamellae.

By this reasoning, the effective size of the titanohematite carrying the remanence perpendicular to c axis (Carmichael, 1961) is between 0.2 and 0.4 mm. This size, according to Kletetschka et al. (2000b), is within a range capable of acquiring intense TRM. Because the magnetization of titanohematite is confined to the plane perpendicular to the c axis, the dissolution of the grain parallel to c axis should not have as significant an effect as the dissolution within the hematite basal plane. This is evident from the

intense NRM of mica-like natural hematite (Kletetschka et al., 2000a) that had their c axes perpendicular to the cleavage plane.

4.2. High REM and coercivity of titanohematite

Kletetschka et al. (2000a) found that coarse-grained Ti-free hematite can acquire a large REM while maintaining relatively low coercive force. Fig. 2 indicates that samples of hematite with variable Ti content also had a large REM. Additionally, these samples show relatively large resistance to AF demagnetization (Fig. 3), and thus, high coercivity, as indicated by the hysteresis loops in Fig. 4. In general, samples with large REM tend to have high coercivity (Fig. 5). This high coercivity and AF resistance contrasts with the low coercivity and AF resistance observed in coarse-grained pure hematite (Kletetschka et al., 2000a,b).

Another difference between coarse-grained pure hematite (Kletetschka et al., 2000b) and the titanohematite, we considered, is that grain size variations, as exemplified by our own analysis of sample w6b, appear to have little effect on AF demagnetization resistance (Fig. 3) and TRM acquisition (Fig. 6). Thus, the acquisition by magnetic remanence for massive, coarse-grained titanohematite resembles that of fine-grained pure hematite.

The reason for this high coercivity and negligible grain size dependence may be related to the exsolution of ferrian ilmenite lamellae. For example, the two micrographs in Fig. 7 show titanohematite that is clearly divided by exsolved ferrian ilmenite lamellae, with spacing of less than $1\text{ }\mu\text{m}$. Schlenger and Veblen (1989) showed in their Fig. 6b that, locally, the spacing between ferrian ilmenite lamellae might be as small as 20 nm. Thus, the effective grain size of the titanohematite must be considered in terms of these microstructures and may not exceed $1\text{ }\mu\text{m}$. In addition, $1\text{ }\mu\text{m}$ -like behavior can be deduced from acquisition curves of grains bearing the same microstructures (Fig. 6). The shape of these curves is identical to those measured for $1\text{ }\mu\text{m}$ fractions of pure hematite (Kletetschka et al., 2000b). Absence of grain size dependence for sample w6b and the large coercivity of titanohematite samples further support the contention that magnetic behavior is controlled by effective grain size not exceeding $1\text{ }\mu\text{m}$.

The remaining question is why these samples have such intense NRM that is not reproducible in laboratory as TRM in a 5×10^{-5} -T field.

4.3. TRM of the Wilson Lake titanohematite

The evidence for large REM values suggests that the titanohematite grain acquires magnetization while it is still homogeneous. The grain behaves like a large mono-mineralic-metastable single domain grain that can acquire a large magnetization (Kletetschka et al., 2000b). As the temperature slowly drops, the exsolution of ilmenite lamellae is activated, thereby locking in the magnetization and producing the microstructure responsible for the high coercivity.

The details of this process can be illustrated with the calculated phase diagram (Burton and Lindsley, 1991) for the hematite–ilmenite system (Fe_2O_3 – FeTiO_3) given in Fig. 9. The diagram shows the titanohematite, ferrian ilmenite, and the disordered hematite–ilmenite solid solution phases. The dependence of the Curie temperature on the titanohematite composition indicates that the hematite-rich region, with up to about 0.15% ilmenite, is homogeneous at the Curie temperature.

This composition is consistent with the rocks from Wilson Lake (Kletetschka, 1998; Kletetschka and

Stout, 1998) that are labeled “Wilson” in Fig. 9. Thus, hematite can acquire magnetization as a large homogeneous titanohematite grain. Its TRM is acquired similarly to that of the pure hematite (Kletetschka et al., 2000b). The subsequent exsolution of ferrian ilmenite lamellae results in the hardening of the initial RM.

4.4. Chemical remanent magnetization (CRM) and/or TRM of the Allard Lake titanohematite

The TRM acquisition mode for the Wilson Lake titanohematite, however, does not hold strictly for the composition of the Allard Lake samples that are rich in ferrian ilmenite. The bulk composition of these rocks (0.71% ilmenite) is labeled “Allard” in the phase diagram (Fig. 9). As the rocks cool, they approach a boundary of continuous reaction where the hemo-ilmenite initiates exsolution lamellae in disordered hematite–ilmenite solid solution (HIL). Lamellae of HIL grow until the system reaches the temperature of the discontinuous reaction where the HIL phase dissolves and produces titanohematite with ferrian ilmenite exsolution lamellae. Outside the HIL lamellae, the ferrian ilmenite-rich phase precipitates lamellae of titanohematite. This process produces the texture of the Allard Lake rocks (Fig. 10) where the large-scale lamellae of titanohematite, produced presumably by the exsolution of the HIL phase, host the much finer ferrian ilmenite lamellae, while the major ferrian ilmenite component hosts small titanohematite lamellae. The ferrian ilmenite lamellae are derived from the onset of terminal reaction $\text{HIL} \rightleftharpoons \text{H} + \text{IL}$ involving the antiferromagnetically ordered hematite-rich solution (H) and the ordered ilmenite structure solution (IL).

The significant NRM of the Allard Lake rocks produces large REM values (Fig. 2) and is due to titanohematite lamellae that exceed 0.2 mm in diameter (Carmichael, 1961). However, these large lamellae have fine exsolution of ilmenite lamellae, causing significant AF resistance and an increase in coercivity (Figs. 2–4) that is characteristic of a fine-grained hematite (Kletetschka et al., 2000b). These results suggest that the large titanohematite lamellae acquired their magnetization before the exsolution of the fine ilmenite lamellae. These 0.2-mm plates were of homogenous phase with high potential for acquiring

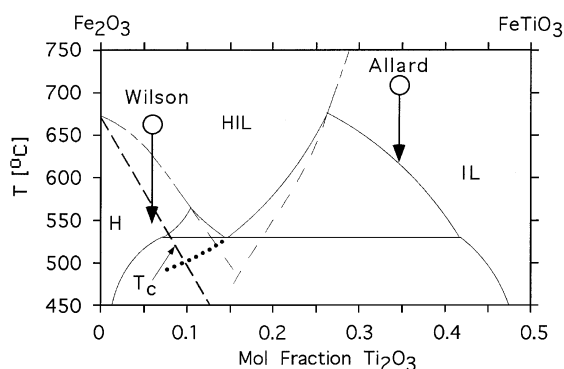


Fig. 9. Part of the calculated phase diagram for the hematite–ilmenite system (Fe_2O_3 – FeTiO_3) after Burton and Lindsley (1991). Labels H, IL and HIL mark the antiferromagnetically ordered hematite-rich solution, ordered ilmenite structure solution, and disordered hematite–ilmenite solid solution, respectively. The labels “Wilson” and “Allard” refer to the hematite-rich and ilmenite-rich sample, respectively. The heavy dotted line represents the metastable exsolution of the HIL phase. The variation of Curie temperature with composition is marked by the curve labeled T_c (Hunt et al., 1995).

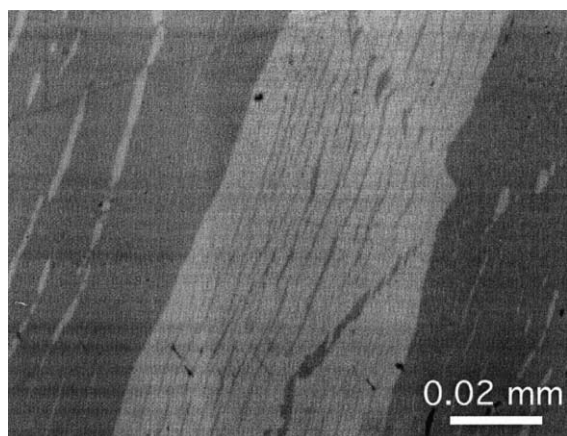


Fig. 10. Photomicrograph of a crystal of hemo-ilmenite cut along the *c* axis from side to side in the polished surface. The broad light gray area contains ilmeno-hematite lamellae with dark gray areas of ferrian ilmenite. Dark gray areas on either side contain hemo-ilmenite with light gray areas of titanohematite.

strong TRM in low external fields (Kletetschka et al., 2000a), and thus capable of developing high REM.

According to the phase diagram in Fig. 9, when the Allard Lake samples cooled, the initial homogeneous ilmenite exsolved and produced the HIL lamellae. These lamellae increased in volume and became more iron-rich. The HIL phase should still be above the Curie temperature when it reached the temperature of discontinuous reaction, and was consumed and replaced by titanohematite with ferrian ilmenite exsolution lamellae (Burton and Lindsley, 1991). By this scenario, the homogeneous 0.2-mm plate of titanohematite never experienced cooling through the Curie temperature because the HIL phase was at higher temperatures (Fig. 9). Therefore, the new titanohematite acquired chemical remanent magnetization (CRM) that is comparable to TRM in intensity (Clark, 1997). The CRM acquired by titanohematite, while it is still homogeneous, seems to be stable during the completion of the exsolution process. However, it is also possible that the large-scale (0.2–0.4 mm) titanohematite lamellae were cooled through the Curie temperature while it was still a homogeneous HIL phase. Hence, the continuous HIL–IL reaction would have continued as a metastable HIL–IL process after cooling through the discontinuous $\text{HIL} \rightleftharpoons \text{H} + \text{IL}$ reaction boundary, as indicated by heavy dotted line in Fig. 9. In this case, the titanohematite would carry the TRM.

5. Conclusions

The source of intense magnetic remanence in rocks carrying titanohematite is within the large titanohematite grains hosting numerous lamellae of ferrian ilmenite that acquire intense RM characterized by large REM (=NRM/SIRM) values. These large REM values are caused by the titanohematite acquiring its TRM as an unmixed ilmeno-hematite phase. The unmixed ilmeno-hematite was cooled through the Curie temperature to acquire the TRM with high REM. In contrast, the hemo-ilmenite rich rock may have acquired CRM during the terminal transformation of the disordered hematite–ilmenite solid solution into titanohematite and ferrian ilmenite. Ferrian ilmenite acquired TRM only if the HIL phase still existed as a metastable phase during cooling through the Curie temperature. Subsequent exsolution of ferrian ilmenite lamellae within the titanohematite hardened the magnetic properties of titanohematite. In general, our observations suggest that the magnetism of the disordered ilmeno-hematite solid solution phase is not significantly perturbed by the continuous ilmeno-hematite \geq titanohematite solid solution reaction.

The intense RM of HISS may be a significant source of the magnetic anomalies obtained from both near-surface and satellite-altitude surveys depending on the extent of the distribution of HISS bearing lithologies. HISS can be found in some plutonic rocks close to those of anorthosite suites, which are rocks characterized by a high abundance of plagioclase feldspar. The crystallization of HISS requires that a relatively high $f\text{O}_2$ attend the crystallization of the magma or recrystallization of metamorphic terrane. Rocks of this nature are found in outcrops that were once part of the lower and middle crust. Hence, the intense RM of HISS may be an important consideration for interpreting magnetic anomalies of the geomagnetic field at any scale.

Acknowledgements

Suggestions by H.C. Noltimier and two anonymous reviewers improved the presentation of this paper. We thank R.B. Hargraves who provided the Allard Lake ilmenite samples and also reviewed an initial draft of this paper. We also thank J.H. Stout, K.

Peterson, K. Kletetschka, M. Kletetschkova and A. Kletetschkova for help with the acquisition of samples from Labrador, Canada.

Appendix A

NRM's were measured with a Superconducting Rock Magnetometer. Samples used were attached to the end of a plastic rod by means of nonmagnetic double-stick scotch tape and measured with the Vibrating Sample Magnetometer equipped with a model 7300 Lake Shore controller. A maximum field of 2 T was supplied by a large water-cooled 12-in. Varian magnet driven by a Tidewater bipolar power supply.

TRM acquisition curves were acquired on cooling from a maximum temperature of 700° in controlled weak fields using a Schoensted Thermal Demagnetizer. The oven was equipped with a cooling chamber containing a conducting coil that enabled the production of an appropriate magnetic field. The magnetic field inside the cooling chamber was measured with a gaussmeter (Bell model 620Z). The probe of this gaussmeter instrument was bent to fit inside the cooling chamber. We tested this modified gaussmeter against a Schonsted Digital Magnetometer to ensure the calibration of magnetic field values. The fields applied during the cooling of our samples ranged from 0.005 to 1 mT. Inside the shielded oven, the smallest field was 0.002–0.003 mT, whereas the maximum acquisition field was 1 mT. Hysteresis properties were measured before and after the thermal treatment to monitor any changes that the air heating would have on the characteristics of the mineralogy of our samples.

References

- Arima, M., Kerrich, R., Thomas, A., 1986. Sapphirine-bearing paragneiss from the northern Grenville province in Labrador, Canada: protolith composition and metamorphic P – T conditions. *Geology* 14, 844–847.
- Banno, S., Kanehira, K., 1961. Sulfide and oxide minerals in schists in the Bessi-Ino district, central Shikoku, Japan. *Jpn. J. Geol. Geogr.* 29, 29–44.
- Brown, E., Raith, M., 1985. Fe–Ti oxides in metamorphic basites from the Eastern Alps, Austria: a contribution to the formation of solid solutions of natural Fe–Ti oxide assemblages. *Contrib. Mineral. Petrol.* 90, 199–213.
- Burton, B.P., Lindsley, D.H., 1991. The interplay of chemical and magnetic ordering. Oxide minerals; petrologic and magnetic significance. *Rev. Mineral.* 25, 303–322.
- Carmichael, C.M., 1959. Remanent magnetism of the Allard Lake ilmenites. *Nature* 183, 1239–1241.
- Carmichael, C.M., 1961. The magnetic properties of ilmenite–haematite crystals. *Proc. R. Soc. London, Ser. A* 263, 508–530.
- Carmichael, C.M., 1964. The magnetization of a rock containing magnetite and hemoilmenite. *Geophysics* XXIX, 87–92.
- Clark, D.A., 1997. Magnetic petrophysics and magnetic petrology: aids to geological interpretation of magnetic surveys. *J. Aust. Geol. Geophys.* 17, 83–103.
- Frost, B.R., Lindsley, D.H., 1991. Stability of oxide minerals in metamorphic rocks. Oxide minerals; petrologic and magnetic significance. *Rev. Mineral.* 25, 469–488.
- Frost, B.R., Lindsley, D.H., Lindsley, D.H., 1991. Occurrence of iron–titanium oxides in igneous rocks. Oxide minerals; petrologic and magnetic significance. *Rev. Mineral.* 25, 433–468.
- Hammond, P., 1952. Allard Lake ilmenite deposits. *Econ. Geol.* 47, 634–649.
- Hargraves, R.B., 1959. Magnetic anisotropy and remanent magnetism in hemo-ilmenite from ore deposits at Allard Lake, Quebec. *J. Geophys. Res.* 64, 1565–1578.
- Hargraves, R.B., Burt, D.M., 1967. Paleomagnetism of the Allard Lake anorthosite suite. *Can. J. Earth Sci.* 4, 357–369.
- Hunt, C.P., Moskowitz, B.M., Banerjee, S.K., 1995. Magnetic properties of rocks and minerals. *Rock Physics and Phase Relations, A Handbook of Physical Constants*. American Geophysical Union, pp. 189–203.
- Kanehira, K., Banno, S., Nishida, K., 1964. Sulfide and oxide minerals in some metamorphic terranes in Japan. *Jpn. J. Geol. Geophys.* 35, 175–191.
- Kelso, P.R., Banerjee, S.K., Teyssier, C., 1993. The rock magnetic properties of the Arunta Block, central Australia and their implication for the interpretation of long wavelength magnetic anomalies. *J. Geophys. Res.* 98B9, 15,987–15,999.
- Kletetschka, G., 1998. Petrogenetic grids and their application to magnetic anomalies in lower crustal rocks, Labrador, PhD thesis, Department of Geology and Geophysics, University of Minnesota, Minneapolis, MN, pp. 157.
- Kletetschka, G., Stout, J.H., 1998. The origin of magnetic anomalies in lower crustal rocks, Labrador. *Geophys. Res. Lett.* 25, 199–202.
- Kletetschka, G., Wasilewski, P.J., Taylor, P.T., 2000a. Hematite vs. magnetite as the signature for planetary magnetic anomalies? *Phys. Earth Planet. Inter.* 119, 265–273.
- Kletetschka, G., Wasilewski, P.J., Taylor, P.T., 2000b. Unique thermoremanent magnetization of multi-domain sized hematite: implications for magnetic anomalies. *Earth Planet. Sci. Lett.* 176, 469–479.
- Langel, R.A., 1985. Introduction to the special issue: a perspective on MAGSAT results. *J. Geophys. Res. Lett.* 9, 243–245.
- Mayhew, M.A., Johnson, B.D., 1987. An equivalent layer magnetization model for Australia based on MAGSAT data. *Earth Planet. Sci. Lett.* 83, 971–981.

- Mayhew, M.A., Johnson, B.D., Wasilewski, P.J., 1985. A review of problems and progress in studies of satellite magnetic anomalies. *J. Geophys. Res.* 90, 2511–2522.
- McEnroe, S.A., 1997. Ilmenite mineral magnetism: implication for geophysical exploration for ilmenite deposits. *Nor. Geol. Surv. Bull.* 433, 36–37.
- McEnroe, S.A., Brown, L.L., 2000. A closer look at remanence-dominated aeromagnetic anomalies: rock-magnetic properties and magnetic mineralogy of the Russell Belt microcline–sillimanite gneiss, northwest Adirondack Mountain, New York. *J. Geophys. Res.* 105, 16,437–16,456.
- Peretti, A., Köpel, V., 1986. Geochemical and lead-isotope evidence for a mid-ocean ridge type mineralization within a polymetamorphic ophiolite complex (Monte del Forno, N. Italy–Switzerland). *Earth Planet. Sci. Lett.* 80, 252–264.
- Reeves, C.V., 1989. Aeromagnetic interpretation and rock magnetism. *First Break* 7, 275–286.
- Schlenger, C.M., 1985. Magnetization of lower crust and interpretation of regional magnetic anomalies: example from Lofoten and Vesterålen, Norway. *J. Geophys. Res.* 90B, 11,484–11,504.
- Schlenger, C.M., Veblen, D.R., 1989. Magnetism and transmission electron microscopy of Fe–Ti oxides and pyroxenes in a granulite from Lofoten, Norway. *J. Geophys. Res.*, B 94, 14,009–14,026.
- Shive, P.N., Fountain, D.M., 1988. Magnetic mineralogy in an Archean crustal section: implications for crustal magnetization. *J. Geophys. Res.* 93B, 12,177–12,186.
- Thomas, A., 1993. Geology of the Winokapau Lake area, Grenville Province, Central Labrador. Geological Survey of Canada, 86 pp.
- Toft, P.B., Haggerty, S.E., 1986. A remanent and induced magnetization model of MAGSAT vector anomalies over West African Craton. *Geophys. Res. Lett.* 13, 341–344.
- Wasilewski, P.J., 1973. Magnetic hysteresis in natural materials. *Earth Planet. Sci. Lett.* 20, 67–72.
- Wasilewski, P., Dickinson, T., 2000. Aspects of the validation of magnetic remanence in meteorites. *Meteorit. Planet. Sci.* 35, 537–544.
- Wasilewski, P., Kletetschka, G., 1999. Lodestone—nature’s only permanent magnet, what it is and how it gets charged. *Geophys. Res. Lett.* 26, 2275–2278.
- Wasilewski, P.J., Mayhew, M.A., 1992. The Moho as a magnetic boundary revisited. *Geophys. Res. Lett.* 19, 2259–2262.
- Wasilewski, P.J., Warner, R.D., 1988. Magnetic petrology of deep crustal rocks—Ivrea Zone, Italy. *Earth Planet. Sci. Lett.* 87, 347–361.
- Wasilewski, P.J., Thomas, H.H., Mayhew, M.A., 1979. The Moho as a magnetic boundary. *Geophys. Res. Lett.* 6, 541–544.
- Williams, M.C., Shive, P.N., Fountain, D.M., Frost, R.B., 1985. Magnetic properties of exposed deep crustal rocks from the Superior Province of Manitoba. *Earth Planet. Sci. Lett.* 76, 176–184.